Article

Current Biology

Multisensory navigational strategies of hatchling fish for dispersal

Highlights

- Hatchling fish elevated buoyancy if confined or deprived of sensations of motion
- Hatchlings also adapted steering to rely strongly on gravity sensing
- Behavioral responses tripled hatchling diffusivity in hydrodynamic simulations

Authors

Allia Lin, Efrén Álvarez-Salvado, Nikola Milicic, Nimish Pujara, David E. Ehrlich

Correspondence

dehrlich@wisc.edu

In brief

Lin et al. investigate how newly hatched zebrafish sense and respond to conditions that limit movement. Based on sensations of water flow, vision, and gravity, hatchlings adjust their body density and swimming behavior in ways that complementarily promote covering ground.

Lin et al., 2023, Current Biology *33*, 4917–4925
November 20, 2023
https://doi.org/10.1016/j.cub.2023.09.070

CellPress

Current Biology

CellPress

Article

Multisensory navigational strategies of hatchling fish for dispersal

Allia Lin,[1,4] Efrén Álvarez-Salvado,[1,4] Nikola Milicic,[1,2] Nimish Pujara,[3] and David E. Ehrlich[1,2,5,*]
[1]Department of Integrative Biology, University of Wisconsin-Madison, Madison, WI 53706, USA
[2]Integrative Biology Graduate Program, University of Wisconsin-Madison, Madison, WI 53706, USA
[3]Department of Civil and Environmental Engineering, University of Wisconsin-Madison, Madison, WI 53706, USA
[4]These authors contributed equally
[5]Lead contact
*Correspondence: dehrlich@wisc.edu
https://doi.org/10.1016/j.cub.2023.09.070

SUMMARY

Animals influence how they disperse in the environment by sensing local cues and adapting how they move. However, controlling dispersal can present a particular challenge early in life when animals tend to be more limited in their capacities to sense and move. To what extent and by what mechanisms can newly hatched fish control how they disperse? Here, we reveal hatchling sensorimotor mechanisms for controlling dispersal by combining swim tracking and precise sensory manipulations of a model species, zebrafish. In controlled laboratory experiments, if we physically constrained hatchlings or blocked sensations of motion through vision and the lateral line, hatchlings responded by elevating their buoyancy and passively moving with faster surface currents. Complementarily, in stagnant water, hatchlings covered more ground using hyperstable swimming, strongly orienting based on graviception. Using experimentally calibrated hydrodynamic simulations, we show that these hatchling behaviors nearly tripled diffusivity and made dispersal robust to local conditions, suggesting this multisensory strategy may provide important advantages for early life in a variable environment.

INTRODUCTION

Natal dispersal, movement from place of birth, allows organisms to track suitable environmental conditions, distribute genes, and collectively overcome local extinction events, ultimately impacting the robustness and evolution of populations.[1] Animals express their quality as dispersers and impact fitness by choosing when and where to move based on information about the environment.[2,3] For some species, influencing dispersal presents acute challenges and opportunities during smaller, weaker juvenile stages, when external forces can dominate movement.[4–8] In these cases, animals that find ways to control dispersal can leverage external forces, mitigate risk while especially vulnerable, and dilute competition when kin can be most dense.[9–11]

Precocious control over dispersal is particularly important for fish. Marine fish can use sensory cues to fight water currents and oppose dispersal, remaining in the safety of their home reef.[12–14] In contrast, some freshwater fish can face urgency to emigrate from their birthplace, as natal habitats quickly deteriorate, remodel, and fragment.[15–17] Capacity to sense the environment and control swimming in early development is best understood for zebrafish, native to the volatile freshwater habitats of the Indian subcontinent, like ponds, streams, rivers, and rice paddies.[18] At the time of hatching, zebrafish can evaluate the local environment through visual, lateral line (water flow), and vestibular (graviception and head acceleration) sensory modalities,[19–23] but their small size and nascent nervous systems severely limit swimming ability.[24,25] It remains unclear if hatchlings sense how they disperse or use this information to meaningfully adapt behavior.

We discovered that zebrafish hatchlings can detect conditions that impede dispersal and make adaptive responses to behavior and body. If we constrained hatchlings or impaired water flow and visual sensation, they elevated buoyancy by enlarging their swim bladders, a gas-filled organ they inflate by gulping air.[26] Consequently, they displaced to the surface where they flowed faster down a custom sluice mimicking natural waterways. Throughout 1 day of swimming under this multisensory impairment, hatchlings gradually swam more vigorously and engaged tighter feedback control to stabilize swimming horizontally, more efficiently covering ground. Labyrinthectomy revealed that stabilizing feedback control requires graviception, suggesting hatchlings regulate graviceptive control of swimming based on combined visual and flow sensation. We estimated the magnitude of effect of these mechanisms on dispersal using agent-based hydrodynamic simulations, finding distinct effects on key dispersal features: emigration and diffusion from siblings.[27] Hatchling adaptations nearly tripled diffusivity in stagnant conditions and primed their bodies for passive dispersal in flows. Together, these data show that zebrafish hatch with innate programs to sense environmental conditions and respond with adaptations that may promote dispersal. We discuss underlying neural mechanisms and potential ecological implications.

RESULTS

We first addressed whether hatchlings can respond to environmental features that impact dispersal. To test the hypothesis that hatchlings sense contexts that limit dispersal, we incubated individual, newly hatched larvae in small (1 mL) wells, as opposed to dishes full of siblings that agitate the water. After 24 h, hatchlings in wells swam near the surface and had significantly enlarged swim bladders, organs they inflate by gulping air to elevate buoyancy (14.1 vs. 12.1 nL for controls, n = 18; Figures 1A and 1B).[26] To disentangle water flow from other features of well rearing, including vessel shape and social isolation, we reintroduced typical flow during well incubation by gentle stirring. Hatchlings in wells exhibited no change to swim bladder volume if flow was restored (12.3 nL, n = 18; Figure 1B), revealing that the lack of water flow was the specific feature that stimulated inflation. We conclude hatchlings can detect and respond to flow reduction by elevating their buoyancy.

To understand how hatchlings responded to chronic flow changes, we lesioned flow-sensitive neuromasts of the lateral line. These collections of superficial hair cells are deflected by flow and exposed to the water, permitting specific ablation by soaking in the ototoxin, copper sulfate.[28–30] In a transgenic line to visualize hair cells (*Tg*[*brn3c:mGFP*]), we applied exterior copper sulfate to lesion the lateral line while sparing internal hair cells (Figures 1C, S1A, and S1B; Video S1). These "flow-blind" hatchlings nearly doubled the volume of their swim bladders at 24 h (23.2 vs. 13.8 nL for controls) and 48 h after lesion (22.7 vs. 12.7 nL), leading to a significant 2%–4% reduction in estimated body density (Figures 1E and S1C–S1E; 24 h: 0.964 vs. 0.992 g/mL; 48 h: 0.961 vs. 0.995 g/mL). Flow-blind hatchlings swam steeply upward significantly more than controls for the first 4 h after lesion (Figure S1F), which may facilitate active buoyancy regulation through gulping air at the surface.[26]

Consistent with elevated buoyancy, flow-blind hatchlings were most likely to be found near the surface (Figure 1F; 92% vs. 17% for controls, n = 12) and were more often rising when tracked swimming in depths of water (Figure 1G, 7.56 concatenated h of tracked motion from 60 flow-blind hatchlings and 9.54 h from 66 controls). Flow-blind hatchlings moved along unique, staircase-like paths, thrusting forward with each bout of swimming, then rising while passive (Figure 1H). When returned to normal conditions, flow-blind hatchlings survived well (89% vs. 93% for controls), recovered neuromast fluorescence consistent with lateral line regeneration,[31] and exhibited typical swimming depth and swim bladder volume 6 days later (data not shown). Given that hatchlings responded similarly to low-flow conditions and ablation of the lateral line, we conclude that they use the lateral line to detect flow reduction and respond with swim bladder inflation.

Hatchlings' buoyancy response to low flow facilitated transport once flow was restored. We hypothesized that the positive buoyancy of hatchlings that responded to low-flow environments would prime them to passively move on surface waters, where flow is fastest, if flow returned.[32,33] To model natural transport in the laboratory, we flowed hatchlings down a gold sluice, a prospecting tool that mimics natural substrates where dense gold particles settle in rivers and streams. We anesthetized larvae to preclude behavioral contributions and isolate biomechanical effects. Flow-blind hatchlings flowed 50% faster down the sluice, confirming the hatchling response to low flow promoted passive transit once water flow was restored (Figure 1I; 7.62 vs. 5.07 cm/s, n = 12).

To test whether control of buoyancy affects dispersal on ecologically relevant spatiotemporal scales, we made three-dimensional (3D) hydrodynamic simulations of active and passive hatchling movements in natural flows (Figure S1G). Hatchlings with larger swim bladders rose while passive (Figure 1J), spent more time at the surface, and moved farther downstream (Figures 1K, 1L, and S1H). Typical hatchlings moved downstream slower than would a passive body at the surface, despite their active swimming, by taking refuge from flows at the substrate. In contrast, flow-blind hatchlings exceeded surface speeds by combining maximal passive movement with active swimming (Figure 1L).

Hatchlings face a trade-off when deciding how to disperse because buoyancy increase impedes diffusion from siblings. We found that deviation from neutral buoyancy made transport more uniform across siblings (Figures 1K and 1L). Movement of typical siblings with approximately neutral buoyancy was superdiffusive, meaning they distributed faster than expected for a random walk (Figure 1L). Distribution of siblings via swimming was compounded by differences in exposure to flow at different swimming depths, emphasizing the importance of natural variation of body density for dispersal (Figures 1B and S1D). After hatchlings had elevated their buoyancy, however, their movement was subdiffusive, with uniform exposure to flow causing siblings to eventually move downstream in a cluster.

Given that hatchlings impacted dispersal by adapting their bodies, we next examined whether routine swimming reflected a propensity to disperse. In stagnant tanks, hatchlings swam strikingly horizontally (Figure 2A). Horizontal swimming would promote active dispersal in natural habitats like lakes and streams with large horizontal span relative to depth. We previously showed hatchlings must actively swim to orient horizontally and counteract the destabilizing effects of flow and gravity.[34] By temporally aligning swim bouts, we found that hatchlings turned toward horizontal when they swam, specifically while they decelerated during each bout (Figure 2B).[35] Therefore, hatchlings actively work to stabilize their swimming horizontally.

We identified the sensorimotor mechanism by which hatchlings swim horizontally and promote dispersal. The orientation of flat bodies of water is reliably informed by the direction of gravity, perhaps more reliably than by light or water flow, and we hypothesized hatchlings steer toward horizontal using the ancient and rapidly developing gravity sense.[36–38] To test this hypothesis, we developed a protocol for bilateral labyrinthectomy to acutely lesion the graviceptive vestibular system. Using this approach, we ablated vestibular hair cells while sparing superficial, flow-detecting hair cells of the lateral line, assessed visually in *Tg(brn3c:mGFP)* hatchlings (Figure 2C). We validated each labyrinthectomy using psychometric testing based on swim response likelihood, finding impaired detection of weak vibratory stimuli (Figure 2D).[39] After lesion, hatchlings swam normally in every respect but direction, moving and orienting isotropically (Figures 2E, 2F, and S2). Lesioned hatchlings spent only 52.0% of their time oriented within 45° of horizontal, approximately at chance, compared with 89.0% for controls.

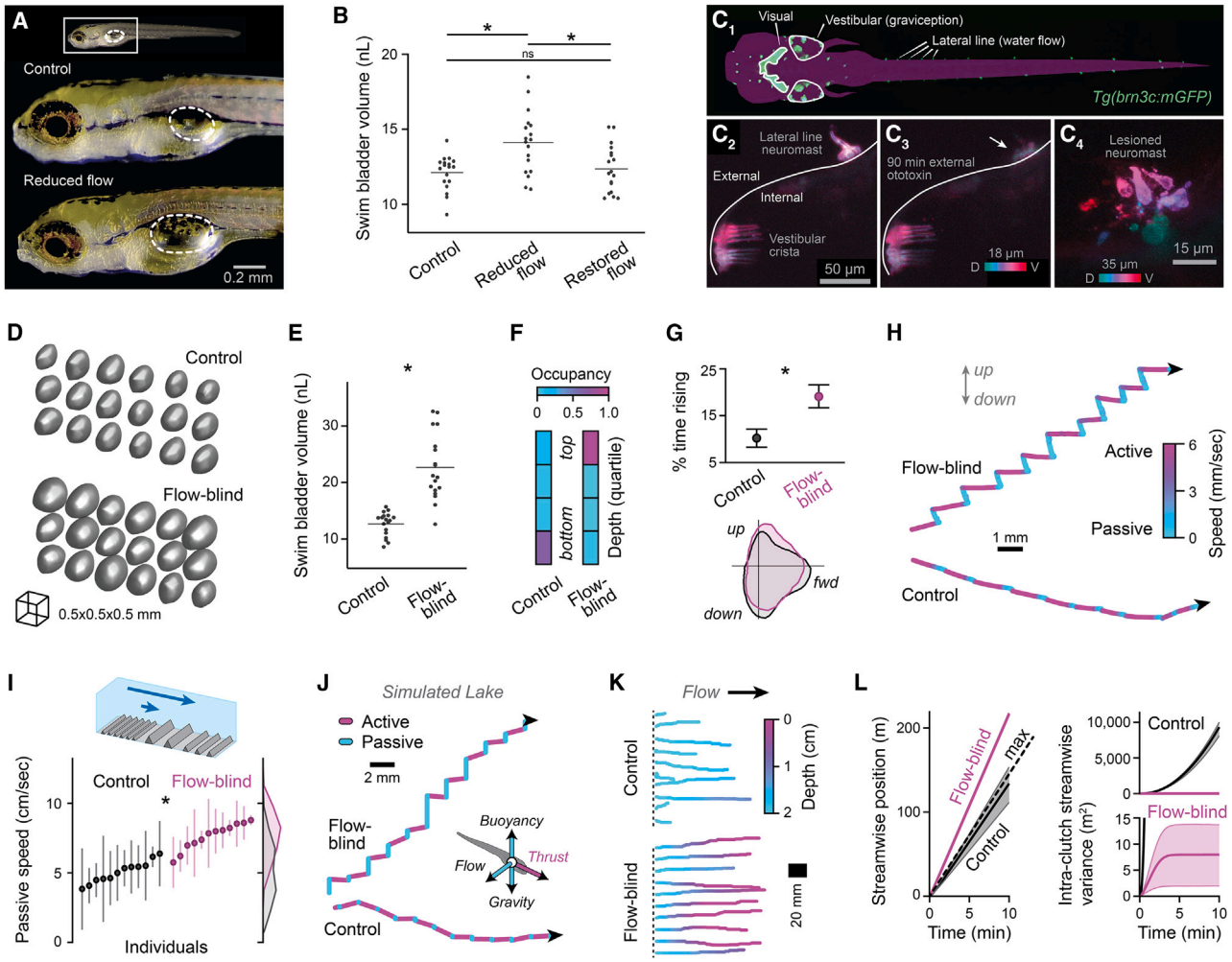

Figure 1. Hatchlings regulate dispersal via body density based on flow conditions

(A) Lateral perspective of a hatchling from a reduced-flow environment and a control sibling, with the extent of the swim bladder outlined.

(B) Swim bladder volume of hatchlings from reduced-flow environments, siblings with flow artificially restored, and control siblings. One-way ANOVA with Bonferroni post-test ($F_{2,51} = 7.85$ *$p < 0.05$ and ns, not significant).

(C) Hair cell responses to lateral line ablation. Dorsal-view photomicrograph of hair cells of lateral line neuromasts and vestibular endorgans, as well as retinal ganglion cells ("visual") in a hatchling of the brn3c:mGFP transgenic line (C1). Confocal, depth-coded projection of a neuromast on the exterior of the otic vesicle and the posterior semicircular canal crista ampullaris interior to the otic vesicle, before (C2) and after (C3) 90 min. external copper treatment. Higher resolution, depth-coded photomicrograph of lesioned neuromast at 35 min. after copper exposure (C4).

(D and E) 3D renderings of swim bladders (D) and measured volumes (E) from flow-blind hatchlings and control siblings 48 h after lesion (n = 18). *$p < 0.05$, two-way ANOVA (see Figure S1), main effect of treatment: $F_{1,68} = 80.8$.

(F) Occupancy of hatchlings in depths of tank by quartile (n = 12). Z test of occupancy at surface: $Z = 3.69$, $p < 0.05$.

(G) Proportion of time freely swimming hatchlings moved upward (top, within 45° of vertical), as mean and bootstrapped 95% confidence interval (CI). Polar probability distributions (bottom) of movement direction while passive (speed below 0.5 mm/s).

(H) Lateral views of swimming paths for one flow-blind hatchling (24 h-post neuromast lesion) and one intact sibling, with instantaneous speed represented as color.

(I) Mean speed in a custom sluice of anesthetized flow-blind and control hatchlings (n = 12), as mean and standard deviation across 3–5 repetitions each. *$p < 0.05$ by two-tailed t test, $t_{22} = 7.16$.

(J) Lateral views of simulated swimming paths with swim bladder volume of a flow-blind and control hatchling. Inset diagram shows forces acting on swimmers in simulation.

(K) Representative paths (top-down) and depth (color-coded) for 10 simulated hatchlings with typical or flow-blind swim bladder volume, swimming for 5 s in shallow, gently flowing water (2 cm/s).

(L) Streamwise position and variance as a function of simulation time for clutches (100 hatchlings) with flow-blind or control swim bladder volumes, shown as mean and 95% CI. Dashed line indicates maximal passive transit at this flow speed.

See also Figure S1 and Video S1.

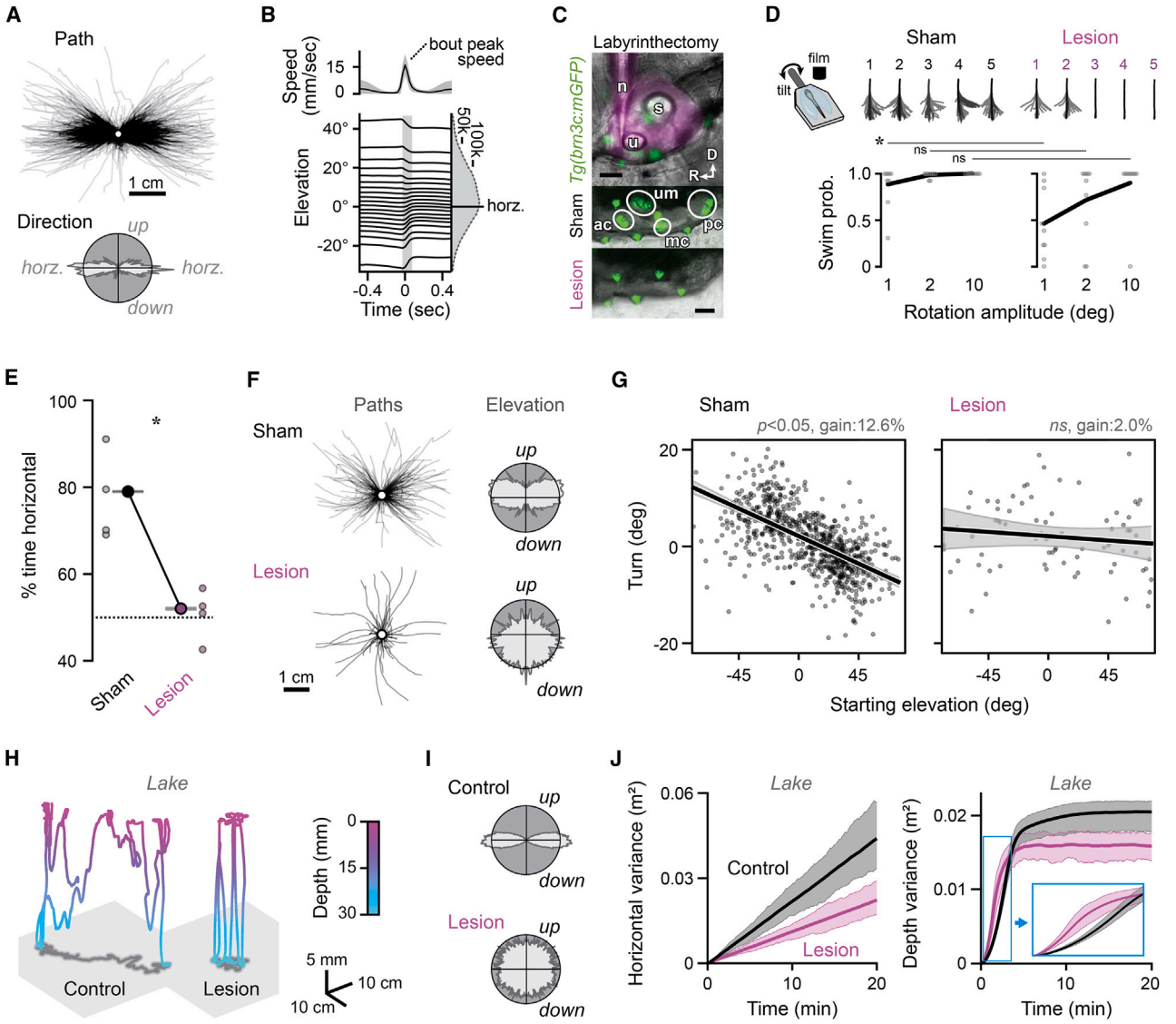

Figure 2. Hatchlings disperse by stabilizing swimming using graviception

(A) Swimming paths (top, n = 1,277) and trajectories (bottom, polar probability distribution) are biased horizontally.

(B) Speed (top, mean ± SD) and elevation (bottom, the body's angle with the horizontal plane) during swim bouts aligned to peak speed. Bouts are sorted into 20 quantiles by pre-bout elevation, and the period of rotation toward horizontal is shaded. Marginal histogram counts frames at each orientation.

(C) Labyrinthectomy via ototoxin pressure injection through a micropipette into the otic vesicle, visualized with sulforhodamine under epifluorescence (magenta, top). Fluorescent inner ear hair cells (circles, *Tg(brn3c:mGFP)*) are lost in lesioned but not sham-injected animals. ac, anterior crista; D, dorsal; mc, medial crista; n, needle; pc, posterior crista; R, rostral; s, saccule; u, utricle; um, utricular macula. Scale bars, 50 μm.

(D) Superimposed tracked tail segments in response to the first 5 rotational stimuli for representative sham and labyrinthectomized (lesion) hatchlings (top). Probability of swim response as a function of stimulus magnitude for individual hatchlings (points) and pooled means (lines). n = 10, *p < 0.05, ns: not significant by two-way ANOVA with Bonferroni post-test.

(E) Proportion of time oriented horizontally (abs. elevation < 45°) during circadian day for groups of sham and labyrinthectomized hatchlings (small points) and pooled data with binomial SD (large points and bars). *p < 0.05, z = 117.5, for 50,898 pooled frames for lesioned hatchlings and 151,705 frames for controls.

(F) Swimming paths and probability distributions of body elevation for sham and lesioned hatchlings.

(G) For individual swim bouts, magnitude of the turn while decelerating (positive is upward, negative downward) is plotted as a function of elevation before the bout. Best-fit lines and 95% confidence intervals are plotted for bouts by sham (n = 791) and labyrinthectomized hatchlings (n = 81).

(H) Simulated 3D swimming paths for one hatchling with an intact graviceptive system (12.6% turn toward horizontal each bout) and one with a labyrinthectomy (0% turn), color-coded by depth.

(I) Polar probability distributions of body orientations of simulated hatchlings with 12.6% gain ("control") vs. 0% gain ("lesion").

(J) Variance of horizontal position (left) and depth (right) in time for 100 siblings in a 30 cm depth of lake as mean and 95% CI.

See also Figure S2.

The graviceptive system stabilized horizontal swimming with high specificity. After lesion, turns during deceleration maintained a similar magnitude but were no longer conditioned on orientation relative to gravity (Figure 2G). Although hatchlings typically turned 12.6% of the way back to horizontal with each swim bout (a stabilizing feedback gain of 0.126), turns were not correlated with orientation in labyrinthectomized hatchlings (gain of 0). The graviceptive system therefore provides a potent, intermittent feedback control mechanism to stabilize horizontal swimming. Control systems of this design elegantly accommodate steering maneuvers that change depth.[35]

The graviceptive system proved critical for dispersal in low-flow conditions. When gravity-blind hatchlings were simulated in a lake, they failed to stabilize horizontally and covered less ground overall, despite swimming at the same intensity and rate (Figures 2H and 2I). Gravity-blind siblings exhibited half the effective diffusivity of intact siblings, distributing less horizontally (Figure 2J). Additionally, intact siblings were slower to distribute throughout the water column but eventually adopted greater depth variance, as they tended to stratify and cover ground near the surface or substrate. Although hatchlings typically direct less of their swimming effort to changing depth than they did without this graviceptive response, they ultimately distributed in depth more effectively. Together, these data mechanistically link the ancient and rapidly developing graviceptive system to dispersal at hatching.

Given the apparent role of swimming stability in dispersal, we tested whether hatchlings can modify stability based on sensory experience. By tracking behavior after loss of flow sensing, we found that hatchlings adjusted swim bout kinematics in parallel to their buoyancy. Specifically, hatchlings adapted by better stabilizing their swimming. By the end of incubation, flow-blind hatchlings in darkness had more than doubled the gain of their stabilizing turns (0.143 vs. 0.068, Figures 3A and 3B). With each swim bout, adapted hatchlings turned more than twice as far toward horizontal. Hatchlings also tended to increase gain following unimodal sensory loss, without either flow sensing (0.131 vs. 0.078) or vision (0.127 vs. 0.100). In contrast, hatchlings failed to adjust their stabilizing gain if their senses were intact (0.084 vs. 0.071). Therefore, hatchlings adapt a stabilizing graviceptive behavior that promotes dispersal based on multimodal sensory feedback.

One possible explanation for swimming adaptation following loss of flow sensing and vision is that hatchlings combine sensory information from both modalities to evaluate motion levels. The lateral line conveys signals not only about external flow but also motion generated by swimming,[40] providing a gross readout of transport. Given that zebrafish can intensify swimming under restraint in virtual reality,[41] we next tested the hypothesis hatchlings swim more vigorously without lateral line or visual sensation. By the end of incubation under multisensory impairment, hatchlings generated bouts of swimming that covered a significantly greater distance (+54.3%, Figure 3C) and lasted significantly longer (+24.2%, Figure S3A). These effects accumulated gradually, with hatchlings swimming an extra 50 μm per bout with each hour (Figure 3D), and for an extra 1.7 ms per bout with each hour (Figure S3B). In contrast, hatchlings with intact senses or unimodal sensory loss did not significantly adapt swimming (Figure 3C), and interbout interval was unaffected by lateral line ablation (Figure S3C), suggesting that lateral line and visual inputs may provide a multisensory calibration signal specifically for swimming vigor.

To understand how these changes to swimming intensity and stability impact dispersal, we compared adapted and unadapted hatchlings in the simulated lake. Hatchlings with greater swimming intensity and stability covered more ground and distributed farther from siblings, nearly tripling their effective diffusivity (268% vs. unadapted swimmers, Figures 3E and 3F). These data confirm that hatchlings can adapt swimming based on sensory feedback to dramatically improve dispersal, making more efficient use of each swim bout by better stabilizing horizontally.

If hatchlings are capable of swimming more intensely and stably, why would they engage in this swimming mode conditionally? Simulations in the river provide an answer, as adapted swimming provided negligible benefit to movement downstream and dispersal from siblings (Figure 3G). In fact, more vigorous swimming was counterproductive for distribution from siblings in flow, countermanding the advantages conferred by individual variation of density within a clutch (Figures S3D and S3E). Together, these data reveal that hatchlings adapt swimming in the absence of sensory feedback confirming movement, reflective of low dispersal conditions. Therefore, hatchlings exhibit a tendency to make swimming more vigorous and stable in stagnant but not flowing water. Based on the observation that adapted swimming improves dispersal in stagnant conditions only, we conclude that hatchlings modify their swimming to improve dispersal efficiently, not in flows where the energetic costs are unjustified.

DISCUSSION

Together, these data reveal that hatchling fish can control how they disperse by adapting their bodies and behavior based on sensory cues. Using a unique modeling approach incorporating detailed, empirically derived swimming kinematics and naturalistic flows, we evaluated how behavioral differences across individuals and states affected dispersal. Hatchling zebrafish made more efficient use of their limited swimming repertoire and nearly tripled their diffusivity by increasing swimming vigor and stability in stagnant conditions, revealing that they could flexibly control dispersal through swimming. Although the spatial scale of active contributions to swimming was relatively small, integration over hours and days would scale these distances to appropriate magnitudes to meaningfully impact ontogenetic habitat and potentially fitness.[10,42–44]

The consequences of active swimming adaptation were amplified through interactions with the background flow. Through small changes in buoyancy, hatchlings were able to maximize their passive transport, akin to how bubble-rafting snails passively cross oceans.[45] Hatchlings elevated buoyancy in response to ablation of the lateral line as well as rearing in a stagnant well, and restoration of flow prevented buoyancy changes, suggesting that hatchlings specifically use flow sensing to regulate buoyancy. Recent studies used similar, isolation-rearing paradigms to investigate social perception and avoidance,[46–50] and although our results suggest that artificial flow can substitute for socially mediated flow of similar magnitude, lateral-line-mediated social perception may suppress

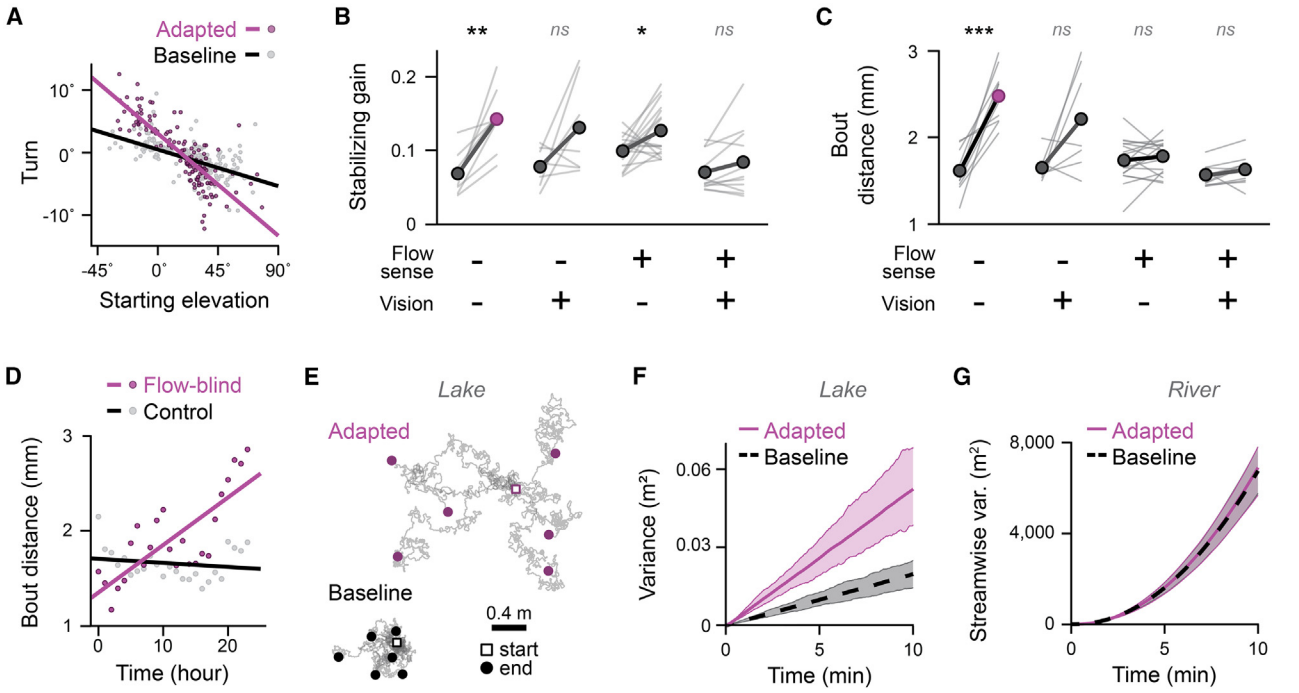

Figure 3. Hatchlings adapt swim intensity and stability to restore dispersal

(A) For discrete swim bouts from one representative clutch, magnitude of the turn while decelerating (positive is upward, negative downward) is plotted as a function of elevation before the bout. Bouts are compared at the start (baseline, n = 189) and end (adapted, n = 132) of swimming in darkness with lesioned lateral line. The slope of the best-fit lines reflects the stabilizing gain (baseline: 0.07, adapted: 0.18).

(B) Stabilizing gain with and without flow and visual sensation (from lateral line lesion and darkness), plotted as paired values for each clutch at the start (left) and end (right) of 28 h of free swimming. Two-way ANOVA, main effect of flow sense: $F_{1,43} = 9.9$, *p < 0.05, **p < 0.005, ns, not significant by paired t test with Bonferroni correction. flow − vision −, n = 10, $t_9 = 5.66$; flow − vision +, n = 8, $t_7 = 2.12$; flow + vision −, n = 18, $t_{17} = 2.85$; flow + vision +, n = 11, $t_{10} = 1.56$.

(C) Swim bout distance plotted as in (B). ***p < 0.0005, ns, not significant by paired t test with Bonferroni correction. Flow − vision −, $t_9 = 6.89$; flow − vision +, $t_6 = 2.56$; flow + vision −, $t_{17} = 1.29$; flow + vision +, $t_9 = 2.09$.

(D) Hourly mean swim bout distance pooled for individuals in darkness in (C), plotted with best-fit lines. R^2 for flow-blind: 0.61, for control: 0.03.

(E) Top-down projection of paths of 6 hatchlings with baseline swim bout distances (1.61 mm) and stabilizing gain (0.07) or those following adaptation (2.48 mm, 0.14 gain), simulated for 1 h in a lake.

(F and G) Variance of horizontal position in a lake (F) and streamwise position in a river (G) as a function of simulation time for clutches (100 hatchlings) with adapted or baseline swimming kinematics, shown as mean and 95% CI.

See also Figure S3.

buoyancy elevation. Simulated hatchlings with elevated buoyancy were more likely to emigrate together, whereas natural variation around neutral buoyancy promoted diffusion, revealing a potential downside of elevating buoyancy, particularly in dense rearing conditions. Acute responses to social cues may interact with mechanisms described here to promote emigration and diffusion from kin simultaneously. In ethological terms, the multisensory adaptations described would be particularly advantageous in the dynamic natural habitats, including ephemeral pools and oxbow lakes, of zebrafish and many freshwater species[18,51]; if motion detection is diminished, for example, in a constraining or evaporating pool that limits flow and swimming efficacy, the behavioral adaptations we observed may prepare hatchlings to maximize survival chances if new channels open or floodwaters arrive.

Elevating buoyancy promoted movement in flows but may also have considerable costs, and consequences for dispersal in the wild are undoubtedly complex. Buoyancy changes were only a temporary response to sensory changes, as hatchlings returned to normal density within days. It remains unclear if restoration of flow and regeneration of the lateral line was causative for recovery or if hatchlings would recover had sensation remained impaired. Consequences of positive buoyancy for predation risk or hunting success, both in terms of the kinematics of prey capture and the ability to track prey across depths, would be transient. Accordingly, hatchlings are not yet preoccupied with hunting due to yolk stores, perhaps reflecting a critical period when dispersal is a higher priority than prey capture and, consequently, adopting positive buoyancy is a viable strategy.[11]

Zebrafish hatched with flexible behavioral programs and requisite neural pathways to control dispersal. Hatchlings efficiently promoted dispersal in stagnant conditions by stabilizing swimming using sensations of gravity for feedback control of orientation, specifically of elevation through rotations in pitch. They turned horizontally while they decelerated, potentially accommodating independent, serial generation of thrust.[35] Hatchlings set the gain of this feedback—how much each swim bout corrected deviations from horizontal—to hyperstabilize swimming based on multisensory visual and lateral line information, revealing an approach that not only improved dispersal in stagnant conditions

but also may generally afford flexible management of trade-offs between stability and maneuverability.[52] These data provide evidence for long-timescale modifications to swimming based on lateral line sensation that complement short-timescale flow responses during rheotaxis[53–55] and long-timescale hormonal changes.[56] Flow stimuli can elicit sustained activity changes in the serotonergic raphe,[57] identifying a potential neural intermediate to transform prolonged flow changes into swimming adaptation as well as integrate flow and visual sensation. Consistently, serotonin can sensitize vestibular reflexes, and serotonergic drugs can impact balance in humans,[58,59] and future tests will address if serotonin directly sensitizes graviceptive stabilization of swimming in hatchlings. Vestibular sensitization could in turn stimulate swim bladder inflation, which requires central vestibular activity, providing a common mechanism for adaptation.[60]

The ability to control dispersal at hatching could have profound consequences for fitness and ecology of freshwater fish. Several examples of larval fish producing informed dispersal come from marine habitats, where older larvae than those studied here oppose dispersal using sensory cues.[13,14] We found that larvae control dispersal earlier in development, within days of fertilization and hatching, and that freshwater fish actively promote dispersal instead of opposing it. Volatile habitats may select for behaviors that promote dispersal,[61] and future studies will be required to evaluate how general these adaptations are across freshwater species or whether they correlate with habitat features. Precocious control over dispersal may confer resilience as habitat volatility increases and fish development accelerates with climate change.[61–63] The behavioral responses we describe for hatchling zebrafish comprise integration across sensory modalities to tailor behavior to local conditions, revealing a strategy for fish to overcome their size and impact how and where they move early in life.

STAR★METHODS

Detailed methods are provided in the online version of this paper and include the following:

- KEY RESOURCES TABLE
- RESOURCE AVAILABILITY
  - Lead contact
  - Materials availability
  - Data and code availability
- EXPERIMENTAL MODEL AND PARTICIPANT DETAILS
- METHOD DETAILS
  - Behavior
  - Sluice
  - Morphometry
  - Confocal microscopy
  - Lateral line lesion
  - Flow manipulation
  - Bilateral labyrinthectomy
  - Swimming simulation
- STATISTICAL ANALYSIS

SUPPLEMENTAL INFORMATION

Supplemental information can be found online at https://doi.org/10.1016/j.cub.2023.09.070.

ACKNOWLEDGMENTS

Research was supported by the National Institute of General Medical Sciences of the National Institutes of Health under award number R35GM146885 to D.E.E. and National Science Foundation grant CBET-2211704 to N.P., as well as a gift from the Wisconsin Alumni Research Foundation. We thank Han Wang for instrument access; Ashwin Bhandiwad, Jesse Weber, Kishore Kuchibhotla, and Tony Ives for helpful feedback; Joel Lord for fabrication; and Mary Halloran and David Schoppik for providing fish lines. This research was performed using the compute resources and assistance of the UW-Madison Center for High Throughput Computing (CHTC) in the Department of Computer Sciences. The CHTC is supported by UW-Madison, the Advanced Computing Initiative, the Wisconsin Alumni Research Foundation, the Wisconsin Institutes for Discovery, and the National Science Foundation, and is an active member of the OSG Consortium, which is supported by the National Science Foundation and the U.S. Department of Energy's Office of Science.

AUTHOR CONTRIBUTIONS

Conceptualization, A.L., E.A.-S., N.P., and D.E.E.; methodology, A.L., E.A.-S., N.P., and D.E.E.; investigation, A.L., E.A.-S., N.M., and D.E.E.; writing, A.L., E.A.-S., N.P., and D.E.E.; visualization, A.L., E.A.-S., and D.E.E.; software, N.P. and D.E.E.; supervision, D.E.E.; funding acquisition, N.P. and D.E.E.

DECLARATION OF INTERESTS

The authors declare no competing interests.

INCLUSION AND DIVERSITY

One or more of the authors of this paper self-identifies as an underrepresented ethnic minority in their field of research or within their geographical location. One or more of the authors of this paper self-identifies as a gender minority in their field of research.

Received: March 14, 2023
Revised: September 26, 2023
Accepted: September 28, 2023
Published: October 20, 2023

REFERENCES

1. Ronce, O. (2007). How does it feel to be like a rolling stone? Ten questions about dispersal evolution. Annu. Rev. Ecol. Evol. Syst. *38*, 231–253. https://doi.org/10.1146/annurev.ecolsys.38.091206.095611.
2. Bowler, D.E., and Benton, T.G. (2005). Causes and consequences of animal dispersal strategies: relating individual behaviour to spatial dynamics. Biol. Rev. Camb. Philos. Soc. *80*, 205–225.
3. Clobert, J., Le Galliard, J.F., Cote, J., Meylan, S., and Massot, M. (2009). Informed dispersal, heterogeneity in animal dispersal syndromes and the dynamics of spatially structured populations. Ecol. Lett. *12*, 197–209.
4. Aleyev, Y.G. (1977). Nekton (Dr. W. Junk).
5. Jenkins, D.G., Brescacin, C.R., Duxbury, C.V., Elliott, J.A., Evans, J.A., Grablow, K.R., Hillegass, M., Lyon, B.N., Metzger, G.A., Olandese, M.L., et al. (2007). Does size matter for dispersal distance? Glob. Ecol. Biogeogr. *16*, 415–425.
6. Benard, M.F., and McCauley, S.J. (2008). Integrating across life-history stages: consequences of natal habitat effects on dispersal. Am. Nat. *171*, 553–567.
7. De Bie, T., De Meester, L., Brendonck, L., Martens, K., Goddeeris, B., Ercken, D., Hampel, H., Denys, L., Vanhecke, L., Van der Gucht, K., et al. (2012). Body size and dispersal mode as key traits determining metacommunity structure of aquatic organisms. Ecol. Lett. *15*, 740–747.
8. Burgess, S.C., Baskett, M.L., Grosberg, R.K., Morgan, S.G., and Strathmann, R.R. (2016). When is dispersal for dispersal? Unifying marine

and terrestrial perspectives. Biol. Rev. Camb. Philos. Soc. *91*, 867–882. https://doi.org/10.1111/brv.12198.

9. Levin, L.A. (2006). Recent progress in understanding larval dispersal: new directions and digressions. Integr. Comp. Biol. *46*, 282–297. https://doi.org/10.1093/icb/icj024.
10. Shurin, J.B., Cottenie, K., and Hillebrand, H. (2009). Spatial autocorrelation and dispersal limitation in freshwater organisms. Oecologia *159*, 151–159.
11. Bonte, D., Van Dyck, H.V., Bullock, J.M., Coulon, A., Delgado, M., Gibbs, M., Lehouck, V., Matthysen, E., Mustin, K., Saastamoinen, M., et al. (2012). Costs of dispersal. Biol. Rev. Camb. Philos. Soc. *87*, 290–312. https://doi.org/10.1111/j.1469-185X.2011.00201.x.
12. Jones, G.P., Planes, S., and Thorrold, S.R. (2005). Coral reef fish larvae settle close to home. Curr. Biol. *15*, 1314–1318. https://doi.org/10.1016/j.cub.2005.06.061.
13. Montgomery, J.C., Jeffs, A., Simpson, S.D., Meekan, M., and Tindle, C. (2006). Sound as an orientation cue for the pelagic larvae of reef fishes and decapod crustaceans. Adv. Mar. Biol. *51*, 143–196.
14. Gerlach, G., Atema, J., Kingsford, M.J., Black, K.P., and Miller-Sims, V. (2007). Smelling home can prevent dispersal of reef fish larvae. Proc. Natl. Acad. Sci. USA *104*, 858–863.
15. Lake, P.S. (2003). Ecological effects of perturbation by drought in flowing waters. Freshw. Biol. *48*, 1161–1172.
16. Lytle, D.A., and Poff, N.L. (2004). Adaptation to natural flow regimes. Trends Ecol. Evol. *19*, 94–100.
17. Lechner, A., Keckeis, H., and Humphries, P. (2016). Patterns and processes in the drift of early developmental stages of fish in rivers: a review. Rev. Fish Biol. Fish. *26*, 471–489.
18. Spence, R., Gerlach, G., Lawrence, C., and Smith, C. (2008). The behaviour and ecology of the zebrafish, Danio rerio. Biol. Rev. Camb. Philos. Soc. *83*, 13–34. https://doi.org/10.1111/j.1469-185X.2007.00030.x.
19. Orger, M.B., Smear, M.C., Anstis, S.M., and Baier, H. (2000). Perception of Fourier and non-Fourier motion by larval zebrafish. Nat. Neurosci. *3*, 1128–1133. https://doi.org/10.1038/80649.
20. Moorman, S.J. (2001). Development of sensory systems in zebrafish (Donio rerio). ILAR J. *42*, 292–298.
21. Ehrlich, D.E., and Schoppik, D. (2019). A primal role for the vestibular sense in the development of coordinated locomotion. eLife *8*, e45839.
22. Liu, Z., Kimura, Y., Higashijima, S., Hildebrand, D.G.C., Morgan, J.L., and Bagnall, M.W. (2020). Central vestibular tuning arises from patterned convergence of otolith afferents. Neuron *108*, 748–762.e4. https://doi.org/10.1016/j.neuron.2020.08.019.
23. Yang, E., Zwart, M.F., James, B., Rubinov, M., Wei, Z., Narayan, S., Vladimirov, N., Mensh, B.D., Fitzgerald, J.E., and Ahrens, M.B. (2022). A brainstem integrator for self-location memory and positional homeostasis in zebrafish. Cell *185*, 5011–5027.e20.
24. Müller, U.K., and van Leeuwen, J.L. (2004). Swimming of larval zebrafish: ontogeny of body waves and implications for locomotory development. J. Exp. Biol. *207*, 853–868. https://doi.org/10.1242/jeb.00821.
25. Pujala, A., and Koyama, M. (2019). Chronology-based architecture of descending circuits that underlie the development of locomotor repertoire after birth. eLife *8*, e42135.
26. Goolish, E.M., and Okutake, K. (1999). Lack of gas bladder inflation by the larvae of zebrafish in the absence of an air-water interface. J. Fish Biol. *55*, 1054–1063. https://doi.org/10.1111/j.1095-8649.1999.tb00740.x.
27. Denny, M. (2016). Ecological Mechanics: Principles of Life's Physical Interactions (Princeton University Press).
28. Linbo, T.L., Stehr, C.M., Incardona, J.P., and Scholz, N.L. (2006). Dissolved copper triggers cell death in the peripheral mechanosensory system of larval fish. Environ. Toxicol. Chem. *25*, 597–603. https://doi.org/10.1897/05-241r.1.
29. Hernández, P.P., Moreno, V., Olivari, F.A., and Allende, M.L. (2006). Sub-lethal concentrations of waterborne copper are toxic to lateral line neuromasts in zebrafish (Danio rerio). Hear. Res. *213*, 1–10. https://doi.org/10.1016/j.heares.2005.10.015.
30. Trapani, J.G., and Nicolson, T. (2010). Physiological recordings from zebrafish lateral-line hair cells and afferent neurons. Methods Cell Biol. *100*, 219–231.
31. Harris, J.A., Cheng, A.G., Cunningham, L.L., MacDonald, G., Raible, D.W., and Rubel, E.W. (2003). Neomycin-induced hair cell death and rapid regeneration in the lateral line of zebrafish (Danio rerio). J. Assoc. Res. Otolaryngol. *4*, 219–234.
32. Koehl, M.A.R., and Cooper, T. (2015). Swimming in an unsteady world. Integr. Comp. Biol. *55*, 683–697. https://doi.org/10.1093/icb/icv092.
33. Huebert, K.B., Cowen, R.K., and Sponaugle, S. (2011). Vertical migrations of reef fish larvae in the Straits of Florida and effects on larval transport. Limnol. Oceanogr. *56*, 1653–1666. https://doi.org/10.4319/lo.2011.56.5.1653.
34. Ehrlich, D.E., and Schoppik, D. (2017). Control of movement initiation underlies the development of balance. Curr. Biol. *27*, 334–344. https://doi.org/10.1016/j.cub.2016.12.003.
35. Ehrlich, D.E., and Schoppik, D. (2017). A novel mechanism for volitional locomotion in larval zebrafish. Preprint at bioRxiv. https://doi.org/10.1101/189191.
36. Liu, Z., Hildebrand, D.G.C., Morgan, J.L., Jia, Y., Slimmon, N., and Bagnall, M.W. (2022). Organization of the gravity-sensing system in zebrafish. Nat. Commun. *13*, 5060.
37. Riley, B.B., and Moorman, S.J. (2000). Development of utricular otoliths, but not saccular otoliths, is necessary for vestibular function and survival in zebrafish. J. Neurobiol. *43*, 329–337. https://doi.org/10.1002/1097-4695(20000615)43:4<329::AID-NEU2>3.0.CO;2-H.
38. Straka, H., and Baker, R. (2013). Vestibular blueprint in early vertebrates. Front. Neural Circuits *7*, 182.
39. Nicolson, T., Rüsch, A., Friedrich, R.W., Granato, M., Ruppersberg, J.P., and Nüsslein-Volhard, C. (1998). Genetic analysis of vertebrate sensory hair cell mechanosensation: the zebrafish circler mutants. Neuron *20*, 271–283. https://doi.org/10.1016/s0896-6273(00)80455-9.
40. Skandalis, D.A., Lunsford, E.T., and Liao, J.C. (2021). Corollary discharge enables proprioception from lateral line sensory feedback. PLoS Biol. *19*, e3001420, https://doi.org/10.1371/journal.pbio.3001420.
41. Ahrens, M.B., Li, J.M., Orger, M.B., Robson, D.N., Schier, A.F., Engert, F., and Portugues, R. (2012). Brain-wide neuronal dynamics during motor adaptation in zebrafish. Nature *485*, 471–477. https://doi.org/10.1038/nature11057.
42. Einum, S., Robertsen, G., Nislow, K.H., McKelvey, S., and Armstrong, J.D. (2011). The spatial scale of density-dependent growth and implications for dispersal from nests in juvenile Atlantic salmon. Oecologia *165*, 959–969. https://doi.org/10.1007/s00442-010-1794-y.
43. Comte, L., and Olden, J.D. (2018). Fish dispersal in flowing waters: a synthesis of movement- and genetic-based studies. Fish Fish. *19*, 1063–1077. https://doi.org/10.1111/faf.12312.
44. Majoris, J.E., Catalano, K.A., Scolaro, D., Atema, J., and Buston, P.M. (2019). Ontogeny of larval swimming abilities in three species of coral reef fishes and a hypothesis for their impact on the spatial scale of dispersal. Mar. Biol. *166*, https://doi.org/10.1007/s00227-019-3605-2.
45. Churchill, C.K.C., Strong, E.E., and Ó Foighi, D.Ó. (2011). Hitchhiking juveniles in the rare neustonic gastropod Recluzia cf. jehennei (Janthinidae). J. Molluscan Stud. *77*, 441–444. https://doi.org/10.1093/mollus/eyr020.
46. Anneser, L., Alcantara, I.C., Gemmer, A., Mirkes, K., Ryu, S., and Schuman, E.M. (2020). The neuropeptide Pth2 dynamically senses others via mechanosensation. Nature *588*, 653–657. https://doi.org/10.1038/s41586-020-2988-z.
47. Groneberg, A.H., Marques, J.C., Martins, A.L., Diez Del Corral, R., de Polavieja, G.G., and Orger, M.B. (2020). Early-life social experience shapes social avoidance reactions in larval zebrafish. Curr. Biol. *30*, 4009–4021.e4. https://doi.org/10.1016/j.cub.2020.07.088.

48. Tunbak, H., Vazquez-Prada, M., Ryan, T.M., Kampff, A.R., and Dreosti, E. (2020). Whole-brain mapping of socially isolated zebrafish reveals that lonely fish are not loners. eLife *9*, e55863, https://doi.org/10.7554/eLife.55863.

49. Anneser, L., Gemmer, A., Eilers, T., Alcantara, I.C., Loos, A.Y., Ryu, S., and Schuman, E.M. (2022). The neuropeptide Pth2 modulates social behavior and anxiety in zebrafish. iScience *25*, 103868. https://doi.org/10.1016/j.isci.2022.103868.

50. Wee, C.L., Song, E., Nikitchenko, M., Herrera, K.J., Wong, S., Engert, F., and Kunes, S. (2022). Social isolation modulates appetite and avoidance behavior via a common oxytocinergic circuit in larval zebrafish. Nat. Commun. *13*, 2573. https://doi.org/10.1038/s41467-022-29765-9.

51. Parichy, D.M. (2015). Advancing biology through a deeper understanding of zebrafish ecology and evolution. eLife *4*, https://doi.org/10.7554/eLife.05635.

52. Webb, P.W., and Weihs, D. (2015). Stability versus Maneuvering: challenges for Stability during Swimming by Fishes. Integr. Comp. Biol. *55*, 753–764. https://doi.org/10.1093/icb/icv053.

53. Oteiza, P., Odstrcil, I., Lauder, G., Portugues, R., and Engert, F. (2017). A novel mechanism for mechanosensory-based rheotaxis in larval zebrafish. Nature *547*, 445–448. https://doi.org/10.1038/nature23014.

54. Olszewski, J., Haehnel, M., Taguchi, M., and Liao, J.C. (2012). Zebrafish larvae exhibit rheotaxis and can escape a continuous suction source using their lateral line. PLoS One *7*, e36661, https://doi.org/10.1371/journal.pone.0036661.

55. Newton, K.C., Kacev, D., Nilsson, S.R.O., Saettele, A.L., Golden, S.A., and Sheets, L. (2023). Lateral line ablation by ototoxic compounds results in distinct rheotaxis profiles in larval zebrafish. Commun. Biol. *6*, 84. https://doi.org/10.1038/s42003-023-04449-2.

56. Venuto, A., Smith, C.P., Cameron-Pack, M., and Erickson, T. (2022). Alone in a crowd: effect of a nonfunctional lateral line on expression of the social hormone parathyroid hormone 2. Biol. Open *11*, https://doi.org/10.1242/bio.059432.

57. Yokogawa, T., Hannan, M.C., and Burgess, H.A. (2012). The dorsal raphe modulates sensory responsiveness during arousal in zebrafish. J. Neurosci. *32*, 15205–15215. https://doi.org/10.1523/JNEUROSCI.1019-12.2012.

58. Miyashita, Y., and Watanabe, E. (1984). Loss of vision-guided adaptation of the vestibulo-ocular reflex after depletion of brain serotonin in the rabbit. Neurosci. Lett. *51*, 177–182.

59. Balaban, C.D. (2002). Neural substrates linking balance control and anxiety. Physiol. Behav. *77*, 469–475.

60. Schoppik, D., Bianco, I.H., Prober, D.A., Douglass, A.D., Robson, D.N., Li, J.M.B., Greenwood, J.S.F., Soucy, E., Engert, F., and Schier, A.F. (2017). Gaze-stabilizing central vestibular neurons project asymmetrically to extraocular motoneuron pools. J. Neurosci. *37*, 11353–11365. https://doi.org/10.1523/JNEUROSCI.1711-17.2017.

61. Kokko, H., and López-Sepulcre, A. (2007). The ecogenetic link between demography and evolution: can we bridge the gap between theory and data? Ecol. Lett. *10*, 773–782. https://doi.org/10.1111/j.1461-0248.2007.01086.x.

62. O'Connor, M.I., Bruno, J.F., Gaines, S.D., Halpern, B.S., Lester, S.E., Kinlan, B.P., and Weiss, J.M. (2007). Temperature control of larval dispersal and the implications for marine ecology, evolution, and conservation. Proc. Natl. Acad. Sci. USA *104*, 1266–1271.

63. Raventos, N., Torrado, H., Arthur, R., Alcoverro, T., and Macpherson, E. (2021). Temperature reduces fish dispersal as larvae grow faster to their settlement size. J. Anim. Ecol. *90*, 1419–1432. https://doi.org/10.1111/1365-2656.13435.

64. Stewart, W.J., and McHenry, M.J. (2010). Sensing the strike of a predator fish depends on the specific gravity of a prey fish. J. Exp. Biol. *213*, 3769–3777. https://doi.org/10.1242/jeb.046946.

65. Xiao, T., Roeser, T., Staub, W., and Baier, H. (2005). A GFP-based genetic screen reveals mutations that disrupt the architecture of the zebrafish retinotectal projection. Development *132*, 2955–2967. https://doi.org/10.1242/dev.01861.

66. Schneider, C.A., Rasband, W.S., and Eliceiri, K.W. (2012). NIH Image to ImageJ: 25 years of image analysis. Nat. Methods *9*, 671–675. https://doi.org/10.1038/nmeth.2089.

67. Thomas, J.M.D., Chakraborty, A., Berson, R.E., Shakeri, M., and Sharp, M.K. (2017). Validation of a CFD model of an orbiting culture dish with PIV and analytical solutions. AIChE J. *63*, 4233–4242. https://doi.org/10.1002/aic.15762.

68. Warboys, C.M., Ghim, M., and Weinberg, P.D. (2019). Understanding mechanobiology in cultured endothelium: a review of the orbital shaker method. Atherosclerosis *285*, 170–177. https://doi.org/10.1016/j.atherosclerosis.2019.04.210.

69. Forman, C.J., Tomes, H., Mbobo, B., Burman, R.J., Jacobs, M., Baden, T., and Raimondo, J.V. (2017). Openspritzer: an open hardware pressure ejection system for reliably delivering picolitre volumes. Sci. Rep. *7*, 2188. https://doi.org/10.1038/s41598-017-02301-2.

70. Nath, T., Mathis, A., Chen, A.C., Patel, A., Bethge, M., and Mathis, M.W. (2019). Using DeepLabCut for 3D markerless pose estimation across species and behaviors. Nat. Protoc. *14*, 2152–2176. https://doi.org/10.1038/s41596-019-0176-0.

71. Mathis, A., Mamidanna, P., Cury, K.M., Abe, T., Murthy, V.N., Mathis, M.W., and Bethge, M. (2018). DeepLabCut: markerless pose estimation of user-defined body parts with deep learning. Nat. Neurosci. *21*, 1281–1289. https://doi.org/10.1038/s41593-018-0209-y.

72. Koehl, M.A.R., Strother, J.A., Reidenbach, M.A., Koseff, J.R., and Hadfield, M.G. (2007). Individual-based model of larval transport to coral reefs in turbulent, wave-driven flow: behavioral responses to dissolved settlement inducer. Mar. Ecol. Prog. Ser. *335*, 1–18. https://doi.org/10.3354/meps335001.

73. Pujara, N., Koehl, M.A.R., and Variano, E.A. (2018). Rotations and accumulation of ellipsoidal microswimmers in isotropic turbulence. J. Fluid Mech. *838*, 356–368. https://doi.org/10.1017/jfm.2017.912.

74. Monthiller, R., Loisy, A., Koehl, M.A.R., Favier, B., and Eloy, C. (2022). Surfing on turbulence: a strategy for planktonic navigation. Phys. Rev. Lett. *129*, 064502. https://doi.org/10.1103/PhysRevLett.129.064502.

75. Spalart, P.R. (1988). Direct simulation of a turbulent boundary layer up to Rþeta= 1410. J. Fluid Mech. *187*, 61–98.

76. Pujara, N., and Liu, P.L.-F. (2014). Direct measurements of local bed shear stress in the presence of pressure gradients. Exp. Fluids *55*, 1–13.

77. Happel, J., and Brenner, H. (1981). Low Reynolds Number Hydrodynamics (Springer). https://doi.org/10.1007/978-94-009-8352-6.

78. Bagnall, M.W., and McLean, D.L. (2014). Modular organization of axial microcircuits in zebrafish. Science *343*, 197–200. https://doi.org/10.1126/science.1245629.

79. Dunn, T.W., Mu, Y., Narayan, S., Randlett, O., Naumann, E.A., Yang, C.T., Schier, A.F., Freeman, J., Engert, F., and Ahrens, M.B. (2016). Brain-wide mapping of neural activity controlling zebrafish exploratory locomotion. eLife *5*, e12741.

STAR★METHODS

KEY RESOURCES TABLE

REAGENT or RESOURCE	SOURCE	IDENTIFIER
Chemicals, peptides, and recombinant proteins		
Copper sulfate	Millipore Sigma	451657; CAS: 7758-98-7
Experimental models: Organisms/strains		
Zebrafish: Tg(brn3c:mGFP)	Xiao et al.[65] (https://doi.org/10.1242/dev.01861)	ZFIN: ZDB-ALT-050728-2
Software and algorithms		
Matlab	Mathworks (https://www.mathworks.com/products/matlab.html)	RRID: SCR_00162
LabView	National Instruments (http://www.ni.com/labview/)	RRID: SCR_014325
Deposited data	Dryad: https://doi.org/10.5061/dryad.ttdz08m4q	

RESOURCE AVAILABILITY

Lead contact

Further information and requests for resources and reagents should be directed to and will be fulfilled by the lead contact, David Ehrlich (dehrlich@wisc.edu).

Materials availability

This study did not generate new unique reagents.

Data and code availability

Data and code for this manuscript are available on Dryad: https://doi.org/10.5061/dryad.ttdz08m4q. Any additional information required to reanalyze the data reported in this paper is available from the lead contact upon request.

EXPERIMENTAL MODEL AND PARTICIPANT DETAILS

Four to eight days post-fertilization (d.p.f.), wild-type zebrafish of the AB strain were used for experiments unless otherwise indicated. Zebrafish larvae do not undergo sexual differentiation by the age of experimentation. For lateral line lesions, five d.p.f. larvae of the *Tg(brn3c:mGFP)* strain were used. In all cases, naturally spawned eggs were collected, cleaned, and maintained at 28°C in E3 solution (0.30 M NaCl, 0.01 M KCl, 0.03 M CaCl2, 0.02 M MgSO4, pH 7.1) on a 14/10 hour light/dark cycle at a density of 50 per 100-mm diameter Petri dish. Larvae without inflated swim bladders at the time of manipulation or measurement were excluded from all experiments. Animal handling and experimental protocols were approved by the University of Wisconsin-Madison College of Letters and Sciences Institutional Animal Care and Use Committee.

METHOD DETAILS

Behavior

Swimming kinematics were measured within the water column, adapted from a previous approach.[34] Briefly, six larvae from a single clutch were filmed in each glass tank (52x45x12 mm, G208,m Azzota Corp.) using a digital camera (GS3U3-23S6M-C, FLIR) with a close-focusing, manual zoom lens (18-108 mm Macro Zoom 7000 Lens, Navitar). The field of view (approx. 2x2 cm) was aligned concentrically with the tank face. Transillumination was provided by a 5W, 940 nm infrared LED backlight (LED World) with aspheric condenser lens and diffuser (ACL5040-DG15-B, ThorLabs), and an infrared filter (43-953) removed reflections from an overhead, white LED strip (6500K, Adafruit). Occupancy as a function of depth quartile was measured in these tanks for 12 larvae, 10 minutes after acclimation, from lateral photographs with a 16 megapixel Sony camera (OnePlus). Four filming setups were mounted in parallel and enclosed within a light-tight box with an exhaust fan to cool to 28°C. Video was acquired at 40 Hz and the framewise position and orientation of larvae in the field-of-view was computed in real-time using the NI-IMAQ vision acquisition environment of LabVIEW (National Instruments). Swim bouts were detected with a 5 mm/sec speed threshold, bout duration was measured as the number

of frames exceeding this threshold, and bout displacement was calculated as the Euclidian distance between positions at the start and end of this window using custom code in Matlab (Mathworks).

Sluice

A custom fish sluice was prepared from a 27.7x1x1 inch (LxWxD) channel of 1/32 inch aluminum, friction fit with a trimmed, commercially available sluice mat designed for gold recovery, with alternating v-shape, square, and Hungarian riffles (ASR Outdoor). The sluice was installed at a 3° decline and room temperature aquarium water was flown down with a submersible pump (PE-1, Little Giant) connected to tubing with an open-jaw C-clamp (Humboldt) to constrain flow rate to 6.33-6.57 mL/sec. Anesthetized larvae were manually added at the top of the sluice with a transfer pipette and transit duration was timed with a stopwatch for 5 repetitions. If a larva took longer than 60 seconds to exit the sluice, which occurred on 8 of 117 trials, the trial was ended, the data point excluded, and the sluice flushed.

Morphometry

Imaging and analysis for morphometry were performed by experimenters blinded to group. Bright-field photomicrographs of orthogonal dorsal and lateral perspectives of larvae were taken using a 12 megapixel iSight camera (Apple) through the ocular of a stereoscope (MZ12, Leica Microsystems). Larvae were immobilized dorsal up in 2% low-melting point agarose (Thermo Fisher Scientific 16520) and photographed before the agar was sliced vertically and rotated for a lateral-view micrograph. Profiles of the larvae and swim bladders were traced manually, and the dorsal and lateral-view tracings were registered using custom MATLAB code, as previously.[34] We evaluated swim bladder morphology and fish density by fitting elliptic cylinders to morphometric measurements following a method adapted from Stewart and McHenry,[64] assuming a swim bladder density of 1.31 mg/mL and tissue density of 1.04 g/mL, as previously.[34]

Confocal microscopy

Fluorescent hair cells in the *Tg(brn3c:mGFP)* line were imaged with a 60x water immersion objective (LUMPLFLN60XW, Olympus) on an inverted confocal microscope (FV1000, Olympus).[65] Time-lapse images were acquired during ototoxin lesions by application of 50 μM copper sulfate (Millipore Sigma) to the bath. Maximum intensity projections and depth-pseudocolored images were created in ImageJ.[66]

Lateral line lesion

Lesions were performed with 60 min soak of *Tg(brn3c:mGFP)* larvae at 5 d.p.f. in a 50 μM solution of copper sulfate (MilliporeSigma) in E3, followed by 3 washes in E3. The lesion dose and timecourse was calibrated with live imaging using confocal microscopy. Swim bladder imaging began after 24 or 48 hour incubation in darkness following lesion. Lesions of animals used subsequently for behavior were confirmed by specific loss of neuromast fluorescence under a fluorescent stereoscope (SMZ-800N, Nikon). Sham-lesioned siblings underwent parallel soak in vehicle, wash steps, and fluorescence microscopy. Behavioral measurements were taken from 6 hatchlings of a single group per tank, starting 1 hour after termination of lesion and continuing for 28 hours. Swimming kinematics were analyzed hourly and compared during blocks at the start to end of this period, comprising 9 hour windows before (start) and after (end) the dark phase of the entrained 14/10 hour light/dark cycle. Clutches were excluded from analysis if they contained insufficient data in either window (fewer than 50 bout distances, 40 interbout intervals, or 3 tracked turn magnitudes for robust linear regression).

Flow manipulation

Larvae were placed into 1 mL of E3 in a round-bottom, deep 96 well plate (V6771, Promega) in darkness in a 28°C incubator for 24 hours. Each well was 0.78 cm in diameter and 3.71 cm deep. A control group of 60 larvae per 100 mm Petri dish was incubated in darkness in parallel. To restore flow during well rearing comparable to the ambient flow created by other hatchlings, half of the well plates were incubated on an orbital shaker under constant, gentle rotation at 35 rpm (3520, Lab-Line). Assuming 1 cm/sec peak swimming speed and ambient fluid velocity in group rearing, we estimated the order of magnitude of flow in the agitated well as the product of well diameter and well angular frequency, which in our case gives ($V \sim R_{well}\omega_{well} \approx 1$ cm/sec).[67,68]

Bilateral labyrinthectomy

Larvae at 5 d.p.f. were anesthetized in 0.2% MS-222 (Syndel) in E3 for 5 minutes, then mounted on their side in 2% low-melting point agarose (Thermo Fisher Scientific 16520) and submerged in anesthetic solution. *Tg(brn3c:mGFP)* larvae were used to visualize vestibular hair cells and confirm lesion. The superficial otic vesicle was visualized on a widefield fluorescent microscope (BX51WI, Olympus) with 20x water immersion objective (XLUMPLFLN20XW, Olympus) under differential interference contrast. A microinjection needle (1.7 μm diameter tip) was prepared on a micropipette puller (P-97, Sutter Instrument) from a borosilicate glass capillary (1B150F-4, World Precision Instruments) and backfilled with 1 mM copper sulfate (MilliporeSigma). For preliminary calibration, the injection solution was filtered (0.22 μm filter, Millex) after incorporation of 128μM sulforhodamine B (Sigma-Aldrich) to visualize the extent of diffusion under fluorescence. With visual guidance and control of a 3-axis micromanipulator (uMp, Sensapex), the pipette was used to puncture the otic vesicle en route to the proximity of the utricular otolith. Injection was produced with 1-5 pulses of 7 msec duration, 45 psi positive pressure to the micropipette, gated by an Openspritzer[69] triggered with custom code in LabVIEW

(National Instruments). Injection was calibrated by sulforhodamine fluorescence filling the otic vesicle and later verified by comparable distension, and lesion quality and larval health were subsequently validated on an individual basis. After injection, the micropipette was removed, the larva freed from agarose and mounted on the contralateral side, and the protocol repeated for the second otic vesicle. Sham surgeries were performed by anesthetizing and mounting siblings identically, but piercing the otic vesicle with an empty and unpressurized microinjection needle. Larvae recovered overnight before visual verification of lesion by loss of green fluorescence in the otic vesicles.

Psychometric verification of labyrinthectomy was performed by mounting each larva in 2% low-melting point agarose (Thermo Fisher Scientific 16520) on the unmirrored side of a galvanometer (GVS011, ThorLabs) and freeing its tail by removing agarose with a scalpel to film swimming. Swims were evoked with vibration of the galvanometer, comprising 5-cycle, 1 kHz sinusoidal motion of varying amplitude presented in descending order, with each amplitude delivered 5 times with a 5 sec inter-stimulus interval. Stimuli were composed in SutterPatch and commanded with D/A converter (dPatch, Sutter Instrument). The tail was illuminated with a 940 nm infrared, 48-LED array (Homyl) and was filmed with an infrared digital camera (BFS-U3-162SM, FLIR) with high-magnification lens (0.50x InfiniStix, Infinity Optical Company). Videos recorded at 400 fps were tracked with 5 equidistant points along the tail using a custom neural network for each larva, trained on 20 frames for 100,000 iterations using DeepLabCut.[70,71] Following stimulus presentation, lesioned and sham larvae were unmounted and grouped into pairs for 48 hours of swim measurement based on similarity of stimulus sensitivity. Swimming was recorded as described above.

Swimming simulation

To test how various manipulations affect hatchling movement in their habitat (primarily rivers, streams, ponds, and lakes), we consider an agent-based model in 2 canonical flow situations: (1) quiescent water mimicking a still lake and (2) open channel flow mimicking rivers and streams. Following standard models for microswimmer motion in flow,[72–74] hatchling motion was modelled as a kinematic sum of the background fluid velocity (u), the hatchling swimming velocity (v_f), and the hatchling settling velocity (v_s).

$$\frac{dx}{dt} = v_f + u + v_s \quad \text{(Equation 1)}$$

For quiescent fluid, the motion reduced to swimming and settling only. For open channel flow, we used the velocity profile calculated from direct numerical simulations of a zero-pressure-gradient flat plate boundary layer[75] that has been shown to match laboratory data of open channel flow.[76] Water depth was varied and constrained hatchling vertical position. The dimensionless velocity profile can be rescaled to various flow rates and water depths; here the ratio of friction velocity to the free stream flow velocity was chosen to be 0.05 based on experimental data.[76] This model captures the essence of the interactions between the hatchlings and ambient flow. We have neglected turbulent fluctuations and flow-induced reorientations based on observations that hatchlings actively maintain orientation (Figure 3).

Settling speed for larvae was calculated from empirical body densities (ρ_p) assuming horizontal orientation following Happel and Brenner[77]:

$$v_s = \frac{(\rho_p - \rho)\, g d_p l_p}{18 \rho \nu} c \quad \text{(Equation 2)}$$

where ρ is the density of water at 28°C (996.3 $kg \cdot m^{-3}$), ν is its kinematic viscosity (1E^{-6} $m^2 \cdot sec^{-1}$), g is gravitational acceleration (9.81 $m \cdot sec^{-2}$), and d_p and l_p are the mean body diameter (3.17E^{-4} m) and length (3.90E^{-3} m), respectively, of the average hatchling. To calculate diameter, height and width were sampled along the length of each hatchling in our morphometric analysis and averaged. From Happel and Brenner,[77] the shape factor was calculated to be c = 0.23 based on the measured aspect ratio (a = 12.31) using:

$$c = \frac{3}{8}\left(\frac{a}{a^2 - 1} + \frac{(2a^2 - 3)\log\left(a + \sqrt{a^2 - 1}\right)}{(a^2 - 1)^{3/2}}\right) \quad \text{(Equation 3)}$$

Each simulated hatchling had ρ_p drawn randomly from empirical values. Eligible density values (in g/mL) for control hatchlings were [0.993, 0.983, 0.976, 0.975, 0.973, 0.973, 0.972, 0.964, 0.964, 0.961, 0.960, 0.957, 0.954, 0.952, 0.949, 0.938, 0.934, 0.926] and for flow-blind hatchlings were [1.011, 1.007, 1.004, 1.001, 1.001, 0.997, 0.994, 0.993, 0.990, 0.989, 0.988, 0.988, 0.987, 0.987, 0.986].

Larval swimming is modelled on empirical behavior, comprised of discrete bouts rather than continuous swimming. Between bouts, larval motion reduced to the background fluid velocity and settling velocity. The timing of swim bouts was governed by a Poisson process.[34] Larval position and orientation were calculated at 25 msec time intervals, the sampling frequency of empirical swimming data. Initiation of a bout occurred stochastically with a probability each time-step of 0.0435, the empirical probability of bout initiation per frame at 40 fps. Each swim bout comprised a fixed displacement applied evenly over 100 msec. Total bout displacement for larvae was typically 1.61 mm and for those adapted to low flow was 2.48 mm. To test the effect of swim bout displacement on sibling dispersal, we varied displacement and estimated the exponent (ξ) and coefficient (κ) for the power law describing variance (σ^2) as a function of time (t) across 5 simulations of 100 siblings each.

$$\sigma^2 = \kappa t^{\xi} \quad \text{(Equation 4)}$$

Where $\xi = 1$, this is a diffusive regime and we calculated the effective diffusivity (D) via $\kappa = 2Dn$, where n is the number of dimensions in which the spreading is happening.

Larval orientation was defined in nautical convention as heading (angle projected on the horizontal plane) and elevation (angle relative to the horizontal plane) at each time-step. Larvae were initialized at random heading and with zero elevation. Simulated larvae never banked based on observations of a strong roll righting reflex, keeping laterally level with respect to gravity.[78] To simplify implementation of constant bank angle, 3D turns while swimming were applied as extrinsic rotations to heading followed by intrinsic rotations in pitch (nose-up/down) that affected elevation but not heading or banking.

Turning behavior directed swim bouts. The direction of swimming velocity during a swim bout was defined by the heading and elevation of the larval body during that bout. Upon initiation of a bout, the larva generated rotations in heading and pitch. The rotation in heading was drawn from a Gaussian distribution (mean 0°, SD 25°) to approximate turns in a monolayer of water.[79] The rotation in pitch was repeated from the previous bout with 0.8 probability to simulate empirical hysteresis, and new rotations were randomly drawn from a Gaussian distribution matching empirical variance (mean 0°, standard deviation 3.80°). Swim bout heading and elevation were defined from larval orientation following these rotations and maintained throughout the duration of the bout. Alternatively, for simulations testing effects of density (Figure 1) but not larval control of orientation, the elevation of each swim bout's velocity was instead randomly drawn from a Gaussian distribution with variance matching that of empirical swim bout elevation (mean 0°, SD 21.90°).

Upon termination of a swim bout, after displacement was applied in the final time-step, the larva generated a pitch rotation towards horizontal. The magnitude of the rotation was drawn from a Gaussian distribution of mean $-w\theta$, where w is the gain of the corrective rotation (0 for labyrinthectomized larvae, 0.126 for controls) and θ is the larva's current elevation. The distribution had a standard deviation of 1.77°, calculated as the square root of the proportion of variance of empirical rotations while decelerating (+25 to +150 msec from bout peak speed) unexplained by pre-bout orientation.[35]

STATISTICAL ANALYSIS

Statistical analysis and quantification were performed using Matlab (MathWorks). All the details of the different analyses performed are detailed in the Results section and in the corresponding figure legends. Where applicable, significance levels were defined by an alpha of 0.05%, unless otherwise indicated.